Small scale Organic Rankine Cycle testing for low grade heat recovery by using refrigerants as working fluids

Emanuele Fanelli[1*], Simone Braccio[2], Giuseppe Pinto[1], Giacinto Cornacchia[1], Giacobbe Braccio[1]

[1] ENEA - Italian National Agency for New Technologies, Energy and Sustainable Economic Development - S.S. Jonica 106 km 419+500, Rotondella 75026, MT, Italy
[2] Politecnico di Bari - Via Amendola 126/b, Bari 70126, Italy

Corresponding Author Email: emanuele.fanelli@enea.it

ABSTRACT

In the last two decades, big efforts have been addressed to investigate new technologies for emissions abatement and oil dependence reduction. Among these, technologies focused on heat recovery from thermal processes or using low grade heat as energy source (i.e. geothermal, solar), have been gained big attention by the scientific community.

In this paper, a small Organic Rankine Cycle (ORC) plant was tested under different operating conditions and by using refrigerants (R245fa) as working fluids. During these first operational tests the plant was operated only in regenerative layout (i.e. heat from hot fluid coming out of the expander, was partially recovered in the regenerator to preheat liquid fluid at the pumping outlet section). The performances of each of them (first law efficiency, exergy efficiency) were evaluated by imposing the expander inlet temperature and the electrical load at the generator. A simple mathematical model, was also used to predict the reference value of each of the parameter investigated.

1. INTRODUCTION

Waste recovery has been gained in the last two decades big attention by scientific community as response at the continuum interest to search new technologies for energy efficiency improvement. This because energy saving is considered to be equal in importance as energy production by renewable sources to meet the CO_2 emission reduction objectives.

Studies directed by U.S. DOE (U.S. Department of Energy) reported that almost 60% of low-temperature waste heat from manufacturing industries is disposed directly to the environment [1]. As widely discussed by [2], opportunities for heat recovery in the manufacturing and process industry are endless. A comprehensive study for the European countries is reported by [2]. The greatest quantity of heat disposed is in the temperature range 60 – 400°C with highest capacity as lower is the temperature.

Among technologies today available for low grade heat recovery and conversion, Stirling Engine [4], thermo-electrical Seebeck-Peltier systems [3], Kalina cycle [4], trilateral flash cycle and ORC [5], they deserve note. While the first ones can be considered as non-commercial applications due to their lower efficiency of conversion or still in the first phase of development, ORC are surely a mature technology. It is well known that these utilities represent the most attractive solution when energy source is low in temperature or limited in thermal power. These machines can be successfully applied in a wide range of the thermal field: for temperature of the thermal source ranging from 90°C to 350°C and for available thermal power between few kW$_{th}$ (micro and mini ORC) to 10 MW$_{th}$ (large geothermal power plant). In general, it can be stated that the most appropriate filed of application of Organic

Rankine Cycle, is that where usual thermal cycles (gas turbine and steam turbine) become economically and thermodynamically unfeasible. Considering a maximum temperature of the thermal source below 200 - 250°C, a near negative thermal efficiency is achieved if open gas turbine cycle is adopted. This because compression work is close to the expansion one. Now if we consider a Rankine cycle with the same temperature limits, a serious of advantages can be achieved: heat exchanges at variable temperature from the hot sink and to the cold one, characterizing Bryton-Joule cycle, are substituted by constant temperature exchanges. Nevertheless, for Rankine cycles, compression is performed in liquid phase making the respective consumption in power negligible. This means that the useful power achievable is close to the expansion one. In this context, among different working fluids adoptable, water is surely the best choice for high temperature heat sources (i.e. saturated cycle in nuclear power plant or ultra-supercritical cycle in coal fired plant), but its thermodynamic properties lead to multistage capital-intensive turbines. If single stage impulse turbines are used, issues related to high supersonic flow at the stator exit (so at rotor inlet) and high peripheral speeds, must be considered. These issues can be partially overcome by using a reaction turbine, but questions related to high volumetric flow rate ratio between out and inlet condition both for impulse and reaction machines, highly influence their efficiency. All this, impose the adoption of highly expensive multi-stage machines. Furthermore, liquid formation during expansion can occur and, generally, more complex plant schemes are required. The above discussed aspects make water unadoptable for low temperature heat sources where simple arrangements and low-cost expanders are imposed by the economic feasibility of these applications. This latter can be successfully achieved by

selecting an appropriate working fluid different from water. Main parameters that greatly influence the performances of the cycle are the molecular complexity, the molecular mass and their critical temperature. Molecular complexity (i.e. number of atoms) impose the shape of the saturation curves on a T-S diagram and so the arrangement of the plant. The higher the molecular complexity, the higher the need of the recuperator to increase the efficiency of the cycle. Heavy molecules such as MDM for siloxanes (236 kg/kmol) and R245fa for refrigerants (134 kg/kmol), are characterized by lower isentropic enthalpy drop - at least one order of magnitude lower - during expansion with significant advantages in terms of turbine design, as discussed before, with respect to water (lower peripheral speeds and lower number of expansion stages).

Highest efficiency of the cycle is reached as its maximum operational temperature approaches the critical temperature of the working fluid adopted. Furthermore, for a given temperature (obviously lower than the respective critical temperature of the fluid) the efficiency is nearly the same independently by the working fluid considered. It must be pointed out that at high temperatures (above 200°C) the volume ratio between outlet to inlet turbine conditions, could be, for some fluids, greater than 100. This means that for those fluids where high difference between evaporation and condensation temperatures exist, high number of expansion stages must be adopted to prevent transonic or supercritical flows. All these aspects are extensively investigated in [8].

Low temperature applications have been worldwide reported for geothermal low-grade heat recovery (120 – 150°C) and for industrial waste heat recovery, while with reference to higher temperature applications, a great number of installations have been documented for solid biomass combustion, heat recovery from gas turbine and ICE exhaust gases and CSP plants. Exhaustive details about these can be found in [2].

Focusing on low temperature applications, intense research activities, as documented by [8], have been registered from 2000 onward: about 2120 publications and 3470 patents from 2000 to 2016, with Italy at the third world position after China and US. This highlights the increased attention towards low-to-medium temperature heat recovery and how ORC technology is today considered a viable solution for power production in this filed. Continuous technological developments are attended in order to promote the diffusion of the technology in several areas such as the automotive field or for small scale domestic CHP. In the first one, heat is recovered by the engine exhaust and/or cooling systems though the unit setup is radically different if compared to the stationary one. In these cases, the economy of production together stringent regulations and requirements (working fluid toxicity and flammability, GWP, ODP, volume occupied by equipment, operative temperature) still contrast with their widespread applications. Nevertheless, it must be noted that if successful is reached in this industrial sector, several new markets can be encouraged such as those related to small-scale CHP. With reference to these latter, a great potential can be expected by distributed cogeneration especially in that case where a capillary natural-gas distribution is actuated. ORC facilities for domestic use show some advantages respect to Stirling engine and MTG: small-scale units (1 – 30 kW) driven by low temperature sources can be used. It must be pointed out that the electrical efficiency in these cases is very low (below 10%) even though the global efficiency (electric and thermal)

remains in the range of 85-90% [2].

In this work, a small ORC based plant was tested and results compared with theoretical ones obtained by a first approach mathematical model. First law and exergy analysis were also performed to evaluate the whole performances of the plant and where main irreversibilities occur.

2. ENEA'S ORC FACILITY

In this section, a brief presentation of the ENEA's ORC facility for low grade heat recovery is given.

The plant layout is depicted in Figure 1, while Figure 2 shows the general arrangement of the laboratory equipment entirely designed and manufactured by ENEA. Two (i.e. T1 and T2) 1 kW_e at 3600 RPM semi-hermetic scroll expander (displacement 14.5 cm^3/rev, volume ratio 3.5) for oil-free gases manufactured by AirSquared, were installed to test different power schemes. These allow to operate by using different refrigerants as working fluid at maximum temperature and pressure of about 175°C and 14.0 bar respectively. Electrical power is instead provided by the two Voltmaster AC (120V, 60Hz) generators magnetically coupled at the expanders. Electrical power was imposed by two electronic DC loads microprocessor controlled. This results in an accurate and fast measurement and display of actual values, as well as an extended operability by many features which wouldn't be realisable with standard analogue technology. For instance, four regulation modes, i.e. constant voltage (CV), constant current (CC), constant power (CP) and constant resistance (CR) are available to control the imposed load.

Plate heat exchangers accurately designed and optimised in term of total transfer area and pressure drops, were used to supply and subtract heat at the various plant sections. The maximum thermal capacity allowable at the evaporator E1 and at the condenser C1 is about 25 kW_{th} for both. Hot sink was feed by hot thermal oil at maximum temperature of 200°C while at the condenser C1, heat was disposed by using water externally cooled by a dry cooler. This latter condition constrains the minimum temperature of condensation to few Celsius degree above the external air temperature.

In order to get a detailed trace of the temperature and pressure profiles vs. time, inlet and outlet sections of each apparatus of the plant (i.e. pump, heat exchangers, expanders) were equipped by pressure (ceramics – accuracy at 25°C +/- 0.5% FS) and temperature (4-wires PT100 – accuracy +/- 0.1% FS) transducers as shown in Figure 1. Working fluid mass flow rate was instead measured by using a Coriolis type mass flow meter (maximum measure error +/- 0.5% of reading), Figure 3 – (a).

Current and voltage signals by AC generators were acquired by using a specific probe designed for the purpose (accuracy +/- 0.5% FS). As instance, a trace of the acquired sinusoidal waveform (220 Vpp, 50Hz) by an oscilloscope at generator terminals during ORC operation, is shows in Figure 3 – (d). All signals were acquired by using the National Instruments® CRIO-9035 (The cRIO-9035 is an embedded controller ideal for advanced control and monitoring applications. This software-designed controller features an FPGA and a real-time processor running the NI Linux Real-Time OS. In field modules arrangement:

n2 NI 9375 16 DI/16 DO module, 30 VDC, 7 µs Sinking DI, 500 µs Sourcing DO, for digital input and output signals (three

way valves control, in field equipment status).

n1 NI 93618 Counter DI module, 0 V to 5 V Differential/0 V to 24 V Single-Ended, 32 Bit, 102.4 kHz (counter features - resolution 32 bit, sample rate 102.4 kHz maximum, timebase accuracy +/- 50 ppm maximum), for expanders rotational speed measurements.

n1 NI9208 16-Channel, ±20 mA, 24-Bit Analog Input Module (accuracy +/- 0.76% of reading - maximum gain error -, 0.04% of range - maximum offset error), for pressure and mass flow rate signals acquisition.

n2 NI9216 8 RTD module, 0 Ω to 400 Ω, 24 Bit, 400 S/s Aggregate, PT100 (accuracy including noise at 25°C +/- 0.2 °C), for temperature measurements.

n1 NI9215 4 AI, ±10 V, 16 Bit, 100 kS/s/ch Simultaneous (accuracy +/- 0.2% of reading - maximum gain error -, 0.082% of range - maximum offset error), for current and voltage measurements.

n1 NI9263 4 AO, ±10 V, 16 Bit, 100 kS/s/ch Simultaneous Module (accuracy +/- 0.35% of reading - maximum gain error -, 0.75% of range - maximum offset error), for pumps PRM and electronic loads controls.) platform programmed in FPGA mode, Figure 3 – (b). About 110 signals (IN/OUT both analog and digitals) were continuously acquired and generated to perform a full control on the experimental machine.
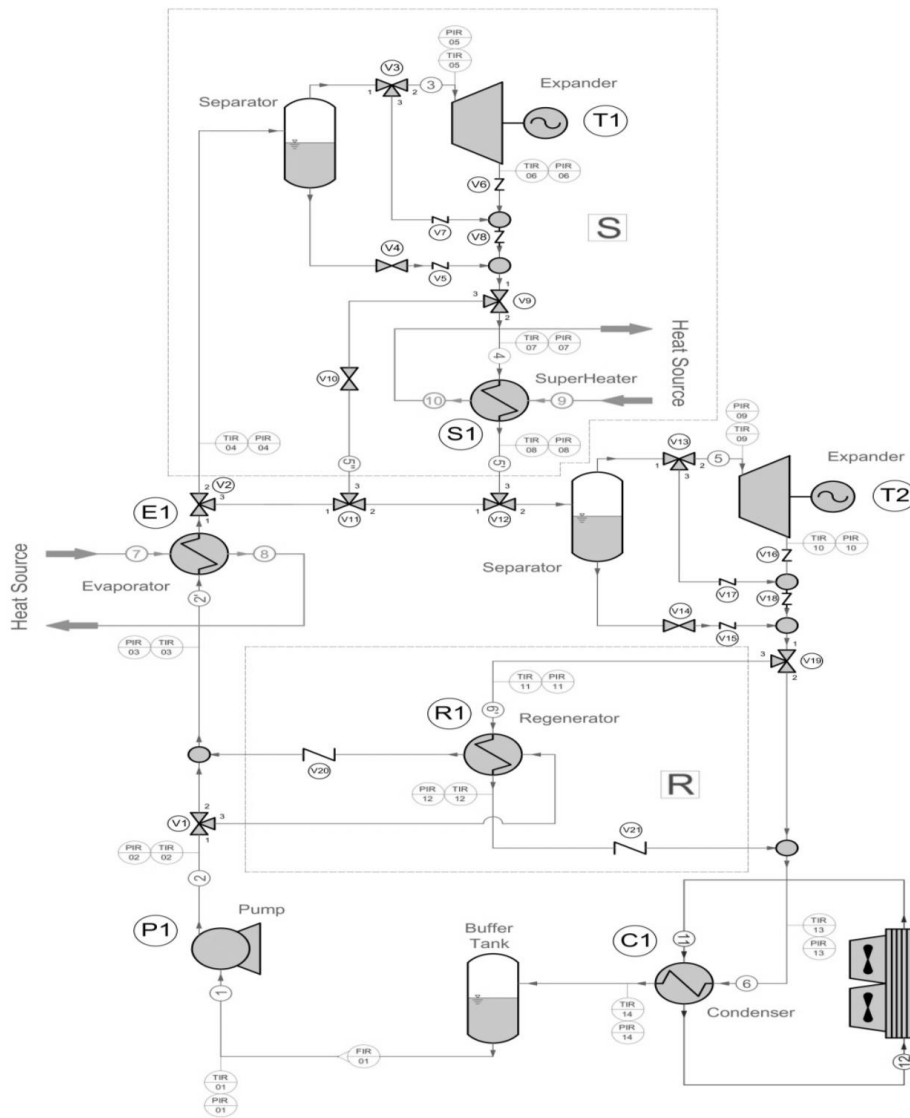

Figure 1. Plant layout

Labview® FPGA module was used to program in FPGA the CRIO controller and to manage all aspects related to the plant operation (embedded Graphical User Interface for data visualization and acquisition, PID and equipment control). Furthermore, CoolProp® libraries and Matlab® scripts were fully integrated inside the Labview® code to perform a real-time evaluation of the cycle performances.

Figure 2. Plant general arrangement
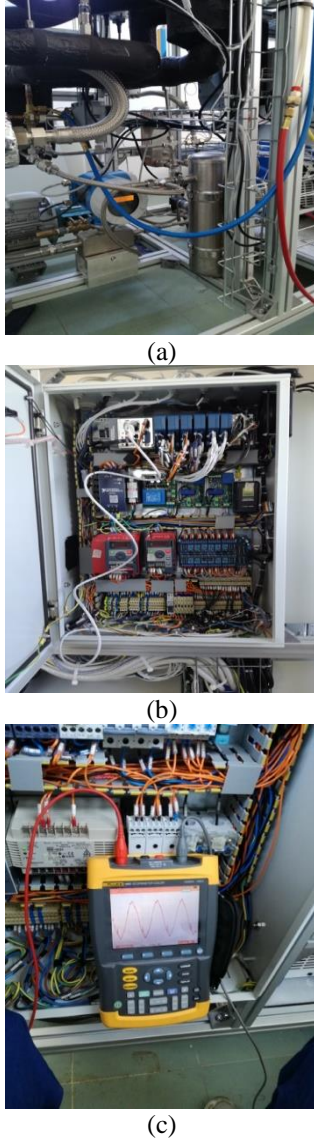
(a)

(b)

(c)

Figure 1. Details of ENEA's ORC facility: a) pumping section where the Coriolis type mass flow meter, buffer tank and pump can be distinguished; b) main system control with NI® CRIO 9035 on the top; c) trace of the sinusoidal 220Vpp 50Hz signal acquired at AC generator terminals during ORC operation

In the following a brief description of the thermal cycle is given with reference to the plant configuration used during the tests: the regenerative one. The working fluid (R245fa in these tests) is stored in the buffer tank at the plant bottom side, where it is sucked by a feeding pump P1 that provide the needed power to allow fluid evolving inside the thermal cycle. At the regenerator R1, the working fluid, still in liquid phase, is preheated by the same fluid - now in vapour phase - coming out of the expander T2.

The phase transition to vapour of the fluid is achieved at the evaporator E1 by using hot thermal oil (Therminol® SP) from the heating section. Here maximum temperature is imposed by a controller (OMRON® type) - operated in feedback mode by using as reference the inlet temperature at the expander T2 - that drives a three-way valve. The high pressure and temperature fluid feed the expander T2 where the required mechanical work is produced. Constant rotational speed of the generator is fixed by a PID that controls the working fluid mass flow rate evolving inside the cycle. At the regenerator

R1, heat from vapour fluid is recovered to preheat the same liquid fluid from the pump P1. At least, heat of condensation is subtracted at the condenser C1 by using cold water. Here the temperature of condensation is controlled by a PID that drive the water circulating pump and the dry cooler fans. The thermodynamic cycle is then closed at the buffer tank where the liquid working fluid is recovered. Safety controls are actuated inside the cycle to avoid pump and expanders failure.

3. MATHEMATICAL MODEL

In this section, mathematical models developed to perform some evaluations of cycle performances are descripted in some details.

3.1 Thermodynamic model

Simple thermodynamic model was developed to get evaluations of the main cycle performances of the experimental facility. Matlab® was used to implement the mathematical code by using CoolProp® libraries to evaluate working fluid properties at each plant sections.

As previously cited, working fluid (R245fa) was stored in the buffer tank where at conditions of temperature T_1 and pressure p_1, it was sucked by the pump P1 that performs an increase in fluid pressure to p_2. The electrical power consumption was evaluated as:

$$\dot{W}_p = \frac{\dot{m}_{wf} \cdot (h_{2,is} - h_1)}{\eta_{is,p} \cdot \eta_{m,p} \cdot \eta_{el,p}} \quad [W] \tag{1}$$

where $\eta_{is,p}$, $\eta_{m,p}$ and $\eta_{el,p}$ are respectively the isentropic, the mechanical and the electrical pump efficiencies (the last one must be more correctly referred to the electric motor that drives the pump). By neglecting thermal losses, the heat recovered by the hot working fluid at the regenerator R1 to preheat the liquid working fluid, can be expressed as:

$$\dot{Q}_{R1} = (h_{2,1} - h_2) = (h_{6,1} - h_6) \quad [W] \tag{2}$$

while that one subtracted at the evaporator E1 from the hot thermal oil, as:

$$\dot{Q}_{E1} = \dot{m}_{wf} \cdot (h_5 - h_{2,1}) = \dot{m}_{oil} \cdot (h_{oil,in} - h_{oil,out}) [W] \tag{3}$$

Properties at the expander T2 inlet section were evaluated once inlet temperature T_5 and pressure p_5 of the fluid were known, while the power produced was calculated by imposing the temperature of condensation and pressure losses along the discharge lines (equivalently by imposing the expansion ratio and the isentropic efficiency of the expander). On the basis of the foregoing assumptions, the electrical power produced was evaluated as:

$$\dot{W}_{el} = \dot{m}_{wf} \cdot (h_5 - h_{6,1,is}) \cdot \eta_{is,e} \cdot \eta_{m,e} \cdot \eta_{el,g} \quad [W] \tag{4}$$

where $\eta_{is,e}$, $\eta_{m,e}$ are respectively the isentropic and the mechanical efficiencies of the expander, while $\eta_{el,g}$ is the electrical efficiency of the generator. At least, the heat disposed at the condenser C1 by cooling water, was assumed to be equal to:

$$\dot{Q}_{C1} = \dot{m}_{wf} \cdot (h_6 - h_1) = \dot{m}_w \cdot (h_{w,in} - h_{w,out}) \quad [W] \quad (5)$$

On the basis of the previous calculations, the first law efficiency was then calculated as following:

$$\eta_I = \frac{\dot{W}_{el} - \dot{W}_p}{\dot{Q}_{E1}} \tag{6}$$

where required in the mathematical model (i.e. to fix the difference of temperature between hot and cold fluids at regenerator R1, at the evaporator E1 and at the condenser C1) temperatures and pressures of the working fluid were assumed to be experimentally derived. This because in the first approach model developed here, there is no modelling of heat exchangers and so there is no prediction of fluid temperature at the exit sections of the heat exchangers.

3.2 Exergy analysis

In every process energy cannot be destroyed but only conserved. Nevertheless, energy balance alone is inadequate for describing some important issues related to energy conversion. For instance, nothing it says about the potential of some energy form to be useful converted to work: all energy in an isolated system must be conserved independently to its final state. Experience shows that irreversibilities inside a system largely destroy this potential so this is finally lower than that at initial system state. A 'property' used to measure this potential of use is exergy. In few words exergy is the maximum theoretical work obtainable by a system when it comes towards to the dead state. It is usual to assume as dead state the normal ambient condition at $T_0 = 293.15$ K e $p_0 = 1$ atm. This means that when a system at initial conditions different from dead state it interacts with the surrounding environment, theoretically work could be available and its maximum is equal to exergy quantity. Unlike energy, exergy is not conserved but it can be destroyed by irreversibilities so an exergy transfer from a system to its surroundings without use represents a loss. The foregoing discussion to introduce the main goal of the exergy analysis: identify inside a system site where exergy is destroyed (i.e. where losses occur) in order to improve the overall performances of the process by mitigating the loss causes. The specific exergy **e** [kJ/kg] of a system can be derived by applying to it the energy and entropy balance:

$$e = (u - u_0) + p_0(v - v_0) - T_0(s - s_0) + \frac{w^2}{2} + gz \tag{7}$$

where u, v, s, w and z are respectively the specific internal energy, volume, entropy, velocity and elevation quote. For a control volume, the exergy rate balance can be expressed as:

$$\frac{dE_{cv}}{dt} = \sum_j \left(1 - \frac{T_0}{T_j}\right)\dot{Q}_j - \left(\dot{W}_{cv} - p_0 \frac{dV_{cv}}{dt}\right) + \sum_i \dot{m}_i e_{f,i} - \sum_e \dot{m}_e e_{f,e} - \dot{E}_d \tag{8}$$

that at steady state is:

$$0 = \sum_j \left(1 - \frac{T_0}{T_j}\right)\dot{Q}_j - \dot{W}_{cv} + \sum_i \dot{m}_i e_{f,i} - \sum_e \dot{m}_e e_{f,e} - \dot{E}_d \tag{9}$$

In the above equations, $\dot{Q}_j$ accounts for the thermal power transfer at the source temperature T_j, $\dot{W}_{cv}$ for the net work transferred by the thermodynamic system, $e_{f,i}$ and $e_{f,e}$ for the

specific exergy associated at the entering mass flow rate $\dot{m}_i$ and exiting mass flow rate $\dot{m}_e$ respectively, $\dot{E}_d$ is the rate of exergy destruction. For a control volume, the specific flow exergy e_f can be expressed in terms of enthalpy as:

$$e = (h - h_0) - T_0(s - s_0) + \frac{w^2}{2} + gz \tag{10}$$

Exergy efficiency of each component was evaluated as in the following. For expander and pump respectively:

$$\varepsilon_{ex,T2} = \frac{\dot{m}_{wf} \cdot (e_{f,T2_o} - e_{f,T2_i})}{\dot{W}_{el}} \tag{11}$$

$$\varepsilon_{ex,P1} = \frac{\dot{W}_{P1}}{\dot{m}_{wf} \cdot (e_{f,P1_o} - e_{f,P1_i})} \tag{12}$$

while for each heat exchanger the following relation was used:

$$\varepsilon_{ex,HE} = \frac{\dot{m}_c \cdot (e_{f,c_o} - e_{f,c_i})}{\dot{m}_h \cdot (e_{f,h_o} - e_{f,h_i})} \tag{13}$$

where $\dot{m}_c$ and $\dot{m}_h$ are the mass flow rate of the cold and the hot fluid respectively, while e_{f,c_j} and e_{f,h_j} are the specific exergy associated at the cold and hot flux respectively at inlet (i) and outlet section (o).

The exergy efficiency of the thermodynamic cycle and the whole plant were evaluated as:

$$\varepsilon_{ex,cycle} = \frac{\dot{W}_{el} - \dot{W}_{P1}}{\dot{m}_{wf} \cdot (e_{E1,wf_o} - e_{E1,wf_i})} \tag{14}$$

$$\varepsilon_{ex,plant} = \frac{\dot{W}_{el} - \dot{W}_{P1}}{\dot{m}_{oil} \cdot (e_{E1,oil_o} - e_{E1,oil_i})} \tag{15}$$

The plant exergy efficiency can be also expressed in term of the efficiency penalties related to the various irreversibility in the power cycle:

$$\varepsilon_{ex,plant} = 1 - T_0 \sum_j \frac{m_j \cdot \Delta S_j}{\dot{m}_{oil} \cdot (e_{E1,oil_o} - e_{E1,oil_i})} \tag{16}$$

where $m_j \cdot \Delta S_j$ is the entropy increase caused by the *j-th* irreversibility.

4. RESULTS

In this section, main results obtained during preliminary tests at the ENEA's ORCLab facility are showed together their comparison with data from mathematical model previously introduced. This allows to get a good comprehension about operational performances of the plant and how main parameters influence the functionality of the machine. In order to evaluate where main irreversibilities are located, results from the exergy analysis are also presented and discussed.

As foregoing introduced, the ENEA's ORCLab facility was designed to allow the conduction of tests on different plant configurations by using different working fluids and by imposing the appropriate operational parameters. The machine was specifically designed to operate with refrigerants at maximum temperature and pressure of 175 °C and 14 bar respectively. During first tests, the ORC was operated in regenerative mode by using R245fa as working fluid. Main

properties of the working fluids successfully adoptable are summarized in Table 1.

Table 1. Main properties of working fluids successfully adoptable at the ENEA's ORC facility

Working fluid	T_c [1] [°C]	p_c [2] [bar]	T_{cond} [3] [°C]	p_{cond} [4] [bar]	GWP[5]
R245fa	153.86	36.51	30.00	1.78	3380
R134a	101.06	40.59	30.00	7.70	3830

Notes: 1. Critical temperature. 2. Critical pressure. 3. Temperature of condensation at pressure p_{cond} (4). 5. GWP at 20 years. All values indicated are derived by CoolProp® library

A representation on the temperature vs. entropy diagram of the thermodynamic transformations that R245fa performs during its evolution inside the ORC machine is showed in Figure 4. In the same figure, main cycle operational points can be easily identified. High pressure transformations are distinguished by low pressure ones by continuous lines against dashed lines respectively.

The fluid at low pressure p_1 and in liquid state (1) is pumped at pressure p_2. Pre-heating occurs inside the regenerator R1 while phase transition to vapour is performed at the evaporator up to reach the maximum cycle temperature T_5 (3).

Here fluid at high pressure and temperature expands up to pressure $p_{4'}$ by producing mechanical work (4). Heat is then recovered by the hot vapor to pre-heat the same fluid in liquid state at the regenerator R1, and finally it is condensed up to temperature T_1 by using cold water (1).

Figure 5, collets main theoretical results obtained by the developed mathematical model. As shown first law efficiency of the cycle was evaluated by varying the main operational parameters.
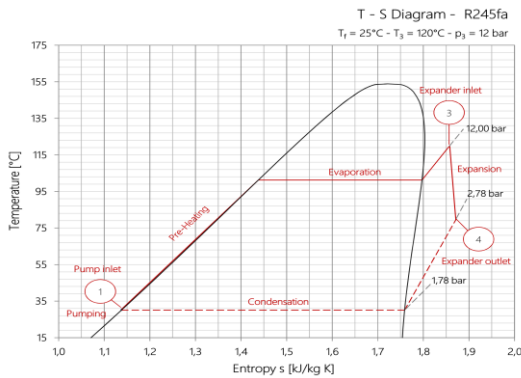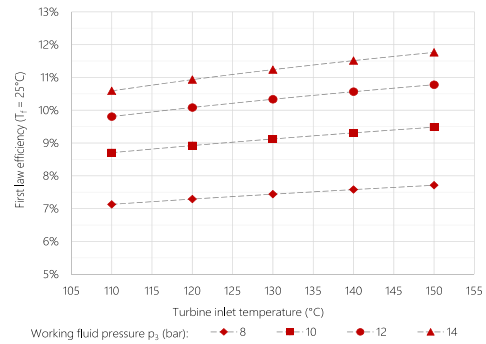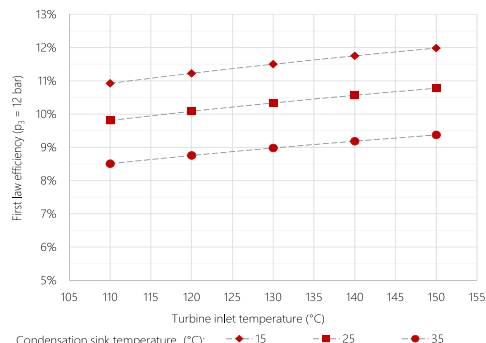

Figure 4. Thermodynamic cycle representation on T-S diagram for R245fa refrigerant

As expected, the efficiency increases, at constant temperature of condensation, as both the temperature and the pressure at the expander inlet increase, Figure 5-(a). The same trend was observed by keeping constant the maximum cycle pressure and by decreasing the cold sink temperature, Figure 5-(b) and (c). This because as lower is the condensing temperature, as lower is the respectively pressure of saturation. In last instance, this increases the pressure drop inside the expander and consequently the produced work at given constant heat introduced inside the thermodynamic cycle. In all numerical cases analysed, the theoretical efficiency was in the range 6% - 12% not very low if compared with the theoretical Carnot efficiency evaluated between the same extreme cycle temperatures (about 21%).
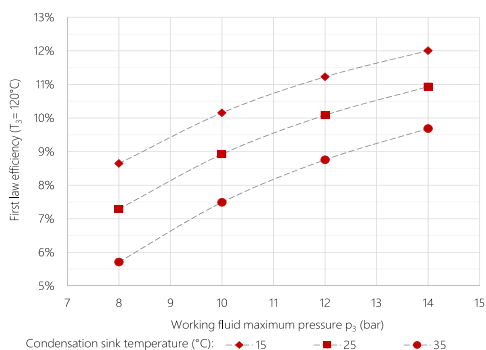
Figure 6 collects main results of the exergetic analysis carried out by considering the following fluid conditions: 115°C and 12 bar respectively as maximum cycle temperature and pressure and 30°C for the condensing temperature. As shown, main irreversibilities are located at the evaporator E1, where about 75% of the introduced exergy, is destroyed, Figure 6-(a). This means that only the residual 25% of the exergy introduced in the cycle, can be useful converted to mechanical work. Because the high difference in temperature between the two fluids, at the evaporator E1, as confirmed by data showed in Figure 6-(c), it is registered the highest exergy destruction rate resulting, in last instance, in a very low exergy efficiency for this component, Figure 6-(b).
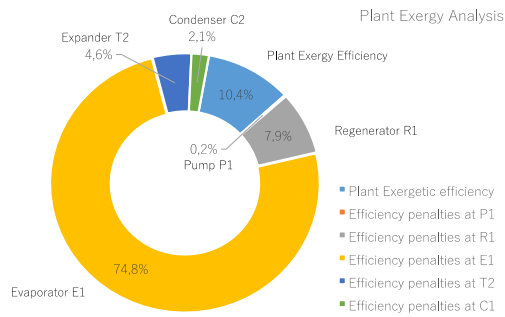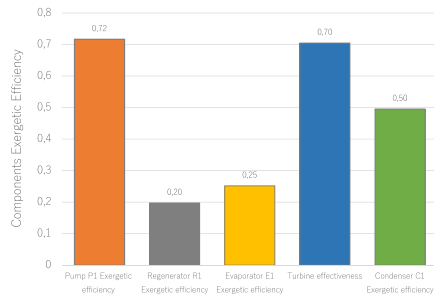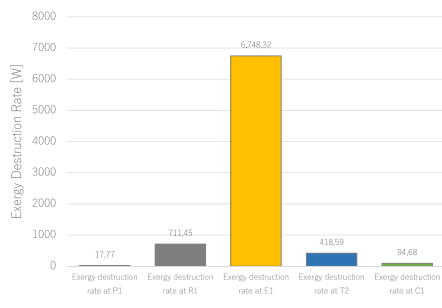

(a)

(b)

(c)

Figure 5. Main theoretical model results. Evolution of the first law efficiency as function: of the inlet expander temperature at varying cycle maximum pressure (T_f constant) (a) and at varying condensing temperature (p_3 constant) (b); of the working fluid maximum pressure at varying condensing temperature (T_3 constant) (c)

(a)

(b)

(c)

Figure 6. Main exergy analysis results: efficiency penalties distribution (a); components exergy efficiency (b); exergy destruction rate at various plant section (c)
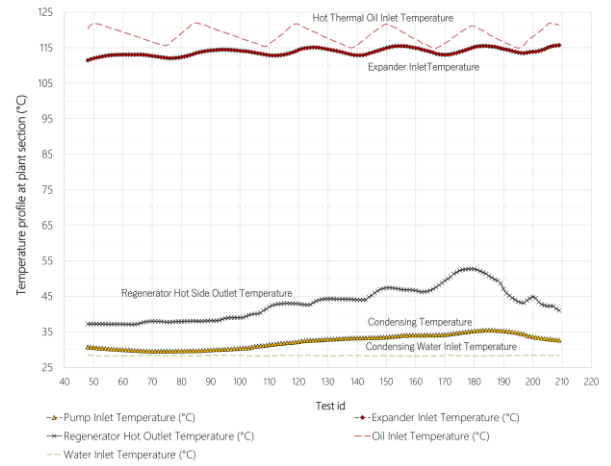
At the condenser, exergy is transferred from the working fluid to condensing water that provide to its final destruction in the subsequent heat transfer towards the environment. The evaluated plant exergy efficiency was about 10.4%, i.e. only 10.4% of the entering plant exergy was useful converted to mechanical work.

A trace of some experimental signals acquired during tests at main plant sections (i.e. expander inlet, regenerator hot side outlet, condenser outlet), is shows in Figure 7 respectively for temperature (a) and pressure (b).
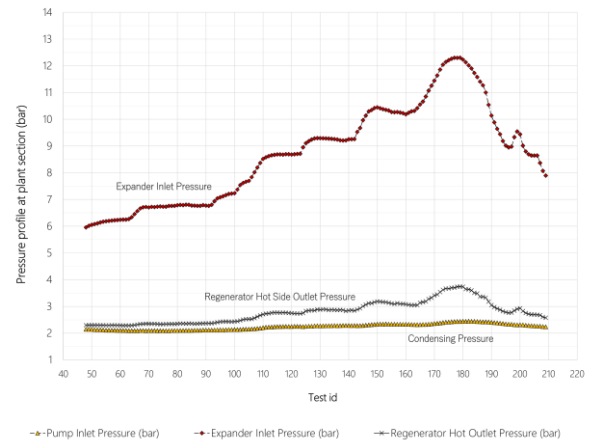
Notable is the increasing in pressure drop at the regenerator hot side that limit the pressure drop available for the expansion at the expander T2. This is largely due at the increased mass flow rate evolving inside the cycle (from about 0.023 kg/s at maximum pressure of 6 bar to 0.048 kg/s at pressure of 12 bar).

Main experimental results by data acquisition elaborations are collected at increasing maximum pressure cycle in TABLE 2 by keeping constant the temperature at the expander inlet and the condensing temperature. Experiments confirm numerical

predictions: efficiency increases as pressure increases. Furthermore, good agreement between experimental data and theoretical ones was observed (Table 3): maximum efficiency registered was 8.4% at maximum inlet pressure at the expander of 10 bar. The deviation by theoretical data is in all cases evaluated below 4%.

(a)

(b)

Figure 7. Some experimental data acquired during tests at the ORCLab: temperature (a) and pressure profiles (b) at the main plant sections (i.e. expander inlet, regenerator hot side outlet, condenser outlet)

Table 2. Main experimental results extracted by acquired data during tests at the ENEA's ORCLab operated in regenerative mode

Reference pressure at inlet expander section	8 bar	9 bar	10 bar
Thermodynamic properties	Experimental Data		
p_1 Inlet pump pressure (bar)	2.16	2.25	2.29
P_2 Outlet pump pressure (bar)	8.67	9.59	10.87
p_5 Inlet expander pressure (bar)	8.02	8.95	9.97
p_6, Outlet expander pressure (bar)	3.62	3.67	3.77
T_1 Inlet pump temperature (°C)	31.07	32.63	33.38
T_2 Oulet pump temperature (°C)	31.40	33.04	34.10
T_2, Inlet evaporator temperature (°C)	68.69	70.46	71.90
T_5 Inlet expander temperature (°C)	113.32	115.04	113.63
T_6, Outlet expander temperature (°C)	91.93	92.77	92.94
T_6 Inlet condenser temperature (°C)	40.36	42.68	43.14
First law efficiency	7.63%	7.91%	8.43%

Table 3. Theoretical vs. experimental data comparison of main results obtained respectively by the mathematical model and acquired during tests at the ORCLab facility operated in regenerative mode

Test pressure	8 bar		9 bar		10 bar	
Th. Properties	Th.	Exp.	Th.	Exp.	Th.	Exp.
p_5 (bar)	8.0	8.0	8.9	8.9	10.0	10.0
T_5 (°C)	113.2	113.2	115.1	115.1	113.6	113.6
$T_{6'}$ (°C)	89.4	91.9	88.8	92.8	83.6	92.9
p_1 (bar)	1.8	2.2	1.9	2.3	2.0	2.3
Efficiency (%)	7.6	7.6	8.1	7.9	8.8	8.4

Notes: p_5 and T_5 pressure and temperature at expander inlet section. $T_{6'}$ temperature at expander outlet section. p_1 pressure at pump inlet (i.e. pressure of condensation).

5. CONCLUSIONS

In this study, a small Organic Rankine Cycle utility (ORCLab - 1 kW_e) for low grade heat recovery was tested by using R245fa as working fluid. In order to increase the overall plant efficiency, the equipment was tested in regenerative mode by imposing the maximum temperature at the expander inlet (115°C) and the electrical load at the generator (i.e. by inducing a variation in the maximum cycle pressure up to 13 bar). Rotational speed was kept constant (3600 RPM) by controlling the working fluid mass flow rate evolving inside the cycle. A first approach thermodynamic model was also developed to predict the performances of the ORC, and main results were discussed in some details. Exergy analysis was also performed to locate main irreversibilities inside the thermodynamic cycle. It was found that about 75% of the entering exergy was destroyed at the evaporator E1. This means that only the residual 25% can be potentially converted in useful work. The evaluated plant exergy efficiency was 10.4%, not low if compared to the ideal Carnot efficiency of a thermodynamic cycle evolving between the same extreme temperature (about 21%). By elaborations of the acquired experimental data, the maximum first law efficiency was 8.43% at maximum cycle pressure of 10 bar and at maximum inlet temperature at the expander of 115°C. Good agreement between theoretical and experimental data was also observed: the maximum deviation was in all cases investigated below 4%.

REFERENCES

[1]   Feng YQ, Hung TC, He YL, et al. (2017). Operation characteristic and performance comparison of organic Rankine cycle (ORC) for low-grade waste heat using R245fa, R123 and their mixtures. Energy Conversion and Management 144: 153–163. http://dx.doi.org/10.1016/j.enconman.2017.04.048

[2]   Piero Colonna, Emiliano Casati, Carsten Trapp and et al. (2015). Organic rankine cycle power systems: from the concept to current technology, applications, and an outlook to the future. Journal of Engineering for Gas Turbines and Power 137: 100801-1-100801-19. https://doi.org/10.1115/1.4029884

[3]   Campana F, Bianchi M, Branchini L, et al. (2013). ORC waste heat recovery in European energy intensive industries: Energy and GHG savings. Energy Conversion and Management 76: 244-252. https://doi.org/10.1016/j.enconman.2013.07.041

[4]   Wang K, Seth R. Sanders, Swapnil Dubey, Fook Hoong Choo, Duan F. (2016). Stirling cycle engines for recovering low and moderate temperature heat: A review. Renewable and Sustainable Energy Reviews 62: 89-108. https://doi.org/10.1016/j.rser.2016.04.031

[5]   Aranguren P, Araiz M, Astrain D, Martínez A. (2017). Thermoelectric generators for waste heat harvesting: A computational and experimental approach. Energy Conversion and Management 148: 680-691. https://doi.org/10.1016/j.enconman.2017.06.040

[6]   Zoltán Varga, Balázs Palotai. (2017). Comparison of low temperature waste heat recovery methods. Energy 137: 1286-1292. https://doi.org/10.1016/j.energy.2017.07.003.

[7]   Pradeep Varma GV, Srinivas T. (2017). Power generation from low temperature heat recovery. Renewable and Sustainable Energy Reviews 75: 402-414. https://doi.org/10.1016/j.rser.2016.11.005

[8]   Macchi E. (2017). Theoretical basis of the organic Rankine Cycle, in Organic Rankine Cycle (ORC) power system. Technologies and Applications, WP Woodhead Publishing – Elsevier 3-22.

[9]   Muhammad Imran, Fredrik Haglind, Muhammad Asim and Jahan Zeb Alvi. (2018). Recent research trends in organic Rankine cycle technology: A bibliometric approach. Renewable and Sustainable Energy Reviews 81: 552-562. https://doi.org/10.1016/j.rser.2017.08.028

NOMENCLATURE

$\dot{E}_d$	Exergy destruction rate [W]
e	Specific exergy [kJ/kg]
g	Gravitational acceleration [m/s^2]
h	Specific enthalpy [kJ/kg]
$\dot{m}$	Mass flow rate [kg/s]
p	Pressure [Pa]
s	Specific entropy [kJ/kg K]
T	Temperature [K]
u	Specific internal energy [kJ/kg]
v	Specific volume [m^3/kg]
$\dot{W}_{cv}$	Net power transferred on the control volume [W]
w	Velocity [m/s]
z	Altitude [m]

Greek symbols

η	Efficiency
ε_{ex}	Exergy efficiency

Subscripts

c	Cold
C1	Condenser C1
e	exit
h	Hot
i	inlet
E1	Evaporator E1
o	Outlet

oil	Thermal oil	T2	Expander T2
P1	Pump P1	w	water
R1	Regenerator R1	wf	working fluid